



Article

In Silico Apple Genome-Encoded MicroRNA Target Binding Sites Targeting Apple Chlorotic Leaf Spot Virus

Muhammad Aleem Ashraf ^{1,2,*,†} , Nimra Murtaza ^{2,†}, Judith K. Brown ^{3,†} and Naitong Yu ^{1,*}

¹ Institute of Tropical Biosciences and Biotechnology, Chinese Academy of Tropical Agricultural Sciences, Haikou 571101, China

² Institute of Biological Sciences, Faculty of Natural and Applied Sciences, Khwaja Fareed University of Engineering and Information Technology, Rahim Yar Khan 64200, Pakistan; nimramurtaza196@gmail.com

³ School of Plant Sciences, The University of Arizona, Tucson, AZ 85721, USA; jbrown@ag.arizona.edu

* Correspondence: ashraf.muhammad.aleem@gmail.com (M.A.A.); yunaitong@163.com (N.Y.)

† These authors contributed equally to this work.

Abstract: *Apple chlorotic leaf spot virus* (ACLSV) (genus, *Trichovirus*; family, *Betaflexiviridae*) is a widespread, deleterious, and the most damaging pathogen of pome and fruit trees including domesticated apple (*Malus × domestica* Borkh.), to which it is transmitted by grafting and pruning. The positive-sense, single-stranded RNA virus is 600–700 nm long and has a genome of 74.7–75.6 kbp in size, minus the poly-A tail and 3′- and 5′-untranslated regions. The genome has three overlapping open reading frames (ORFs) that encode a replication-associated protein (Rep), movement protein (MP), and coat protein (CP). RNA interference (RNAi)-mediated antiviral defense in eukaryotes has evolved to control infections in plant viruses. The objective of this study was to analyze locus-derived microRNAs (mdm-miRNAs) in the apple genome with potential for targeting ACLSV +ssRNA-encoded mRNAs, using a predictive approach that involves four algorithms. The goal is to mobilize the in silico-predicted endogenous mdm-miRNAs and trigger the RNAi pathway experimentally in apple trees to evaluate antiviral resistance to ACLSV. Experimentally validated apple ($2n = 2X = 34$) mdm-miRNAs ($n = 322$) were obtained from the miRBase database and aligned to the ACLSV genome (KU870525). Of the 322 targeting mature locus-derived mdm-miRNAs analyzed, nine apple mdm-miRNA homologs (mdm-miR395k, mdm-miR5225c, and mdm-miR7121 (a, b, c, d, e, f, g, h)) were predicted by all “four algorithms”, whereas fifty-eight mdm-miRNAs were identified as consensus binding sites by the combined results of two algorithms. The miRanda, RNA22, and TAPIR algorithms predicted binding of mdm-miR395k at nucleotide position 4691 and identified it as the most effective interacting mdm-miRNA targeting the virus ORF1 sequence. An integrated Circos plot was generated to validate the accuracy of target prediction and determine if apple mdm-miRNAs could bind to the predicted ACLSV mRNA target(s). A genome-wide in silico-predicted miRNA-mediated target gene regulatory network was implicated to validate interactions necessary to warrant in vivo analysis. The availability of validated locus-derived microRNAs (mdm-miRNAs) with predicted potential to target ACLSV in infected apple trees represents the first step toward development of ACLSV-resistant apple trees.

Keywords: *Trichovirus*; in silico tools; *apple chlorotic leaf spot virus*; miRNA; RNA interference



Citation: Ashraf, M.A.; Murtaza, N.; Brown, J.K.; Yu, N. In Silico Apple Genome-Encoded MicroRNA Target Binding Sites Targeting Apple Chlorotic Leaf Spot Virus. *Horticulturae* **2023**, *9*, 808. <https://doi.org/10.3390/horticulturae9070808>

Academic Editors: Sherif M. Sherif and Laila Ikase

Received: 4 May 2023

Revised: 4 July 2023

Accepted: 11 July 2023

Published: 14 July 2023



Copyright: © 2023 by the authors. Licensee MDPI, Basel, Switzerland. This article is an open access article distributed under the terms and conditions of the Creative Commons Attribution (CC BY) license (<https://creativecommons.org/licenses/by/4.0/>).

1. Introduction

The cultivated apple (*Malus domestica* Borkh.) is an economically and culturally popular fruit and among the most widely produced in the world [1–3]. The first whole genome reference for domesticated apple ($2n = 2X = 34$) was released in 2010 [4]. *Apple chlorotic leaf spot virus* (ACLSV) is a member of the genus *Trichovirus* (family *Betaflexiviridae*). The ACLSV is an economically important, highly damaging, graft-transmissible latent pathogen that occurs worldwide, and infects woody cultivated, ornamental, and wild plants including

apple trees [5–9]. The virus has a positive-sense, single-stranded RNA genome encapsidated in a particle 600–700 nm in length. The ACLSV genome is 74.7–75.6 kbp in size, not including the poly-A tail and the 3′- and 5′-untranslated regions. The genome encodes three overlapping open reading frames (ORFs) from which the viral replication-associated protein (Rep), movement protein (MP), and coat protein (CP) are encoded [10–12].

In plants, microRNAs (miRNAs) have multiple critical roles in various biological processes such as development, growth, response to environmental stress, and to host–virus interaction by controlling gene expression and regulation. They are usually 20–24 nucleotides long and can bind to complementary sequences in messenger RNAs (mRNAs), leading to mRNA degradation or translation repression [13,14]. Plant miRNAs are formed from miRNA precursors (called pri-miRNAs). The enzyme Dicer-like1 (DCL1), ribonuclease (RNase) III, is responsible for processing pri-miRNA transcripts into precursor miRNAs (pre-miRNAs). The DCL cleaves the pri-miRNA stem-loop, releasing a double-stranded RNA molecule containing the miRNA sequence. Subsequently, intermediate duplexes (miRNA/miRNA*) are formed, stabilized, and incorporated into the RNA-induced silencing complex (RISC), which guides the miRNA to the target mRNA through base pairing, resulting in repression [15–18].

The processes involved in microRNA-directed RNA silencing are based on RNA interference (RNAi) and represent a conserved innate defense mechanism in eukaryotes, including plants, for combatting viruses by altering host–virus interaction and inhibiting virus replication [19–21]. Artificial microRNA (amiRNA) can trigger gene silencing that in turn can confer resistance or tolerance in plants to combat invading viruses. The use of amiRNA has been to confer resistance in rice plants to rice stripe virus [22] and in cucumber plants to cucumber green mottle mosaic virus [23] in economically important plants. Apple tree was screened for possible multiple molecular mechanisms to explore mature miRNAs, which are a natural source of immunity to biotic and abiotic stresses and are important for growth and development [24–28]. The apple genome was mapped with experimentally verified 322 mature mdm-miRNAs available in miRBase [29]. The mdm-miRNAs are assumed to have binding sites in the ACLSV genome with high confidence.

In this study, an integrated bioinformatics approach was investigated to predict apple genome-encoded mdm-miRNAs implemented to target the +ssRNA-encoded genome of ACLSV. In silico predicted tools can aid in evaluating how miRNA binding sites interact with different target mRNA. Several publicly available computational analysis algorithms have been developed for predicting miRNA targets. The application of various computer-aided miRNA prediction tools with multiple functions has facilitated in silico prediction in biotechnology, including the development of virus-resistant or -tolerant plants. In this study, several miRNA prediction tools were evaluated and used to identify microRNA–mRNA binding sites in the ACLSV genome for use in developing transgenic or non-transgenic modified apple plants with resistance to ACLSV and, potentially, closely related trichoviruses. Potential targets of the most promising apple miRNAs for breeding were also of interest to better understand trichovirus–apple plant interaction during infection. Until now, there have been no reports of the use of an amiRNA-based strategy to develop ACLSV tolerance in apple plants, which is based on the prediction of homologous amiRNAs for silencing ACLSV.

The objective of this study was to identify the predicted target sites of apple locus-derived mdm-miRNAs and the dynamic miRNA–mRNA target site interactions most likely to result in gene silencing of ACLSV for the future development of virus-resistant, transgenic apple plants.

2. Materials and Methods

2.1. Apple Mature MicroRNAs and ACLSV Genomic Data Source

The available 322 mature apple miRNA sequences (mdm-miRNA156–mdm-miR11020) (accession IDs: MIMAT0025867–MIMAT0043631) were downloaded and available in the miRBase database (version 22) (<http://mirbase.org/> accessed on 26 October 2022) [29]. The

mature sequences of locus-derived mdm-miRNAs in the apple genome were acquired for analysis (Supplementary Table S1). The whole genome sequence (7545 bases) of ACLSV (isolate, SY03) (accession number KU870525) was retrieved from the NCBI (National Center for Biotechnology Information) GenBank database [30].

2.2. Analysis of Multiple mdm-miRNA Target-Pairs in ACLSV Genome

To identify (predict) the mdm-miRNAs likely to bind most efficiently to the ACLSV genome, a predictive approach was used involving four different algorithms most widely used in similar studies to analyze “miRanda, RNA22, TAPIR and psRNATarget” (Table 1). The mature sequences of the apple genome-encoded mdm-miRNAs and the genomic transcript of ACLSV (in FASTA format) were similarly analyzed.

Table 1. Summary of the in silico prediction tools used in this study.

Algorithms	Parameter	Features	Availability
miRanda	Score threshold = 140, Free energy = −20 Kcal/mol, Gap open penalty = −9.00 Gap extend penalty = −4.00	Seed-based interaction, Target site accessibility, free energy of RNA-RNA duplex, conservation	http://www.microrna.org/ (accessed 26 January 2023) [31,32]
RNA22	Folding energy = −15 Kcal/mol Number of paired-up bases = 12, Sensitivity (63%), Specificity (61%),	Non-seed-based interaction, Site complementarity, Target site multiplicity, Pattern recognition, Folding energy of heteroduplex	https://cm.jefferson.edu/rna22/Interactive/ (accessed on 22 October 2022) [33,34]
TAPIR	Free energy = −20 Kcal/mol, Hit per target = 1	Seed paring, Free energy of duplex, Multiple target sites,	http://bibiserv.techfak.uni-bielefeld.de/mahybrid (accessed on 9 November 2022) [35]
psRNATarget	Expectation Score = 6.5, HSP size = 19, Penalty for G:U pair = 0.5 Penalty for opening gap = 2	Multiplicity of target site, Translation inhibition, Target accessibility, Complementarity scoring	https://www.zhaolab.org/psRNATarget/analysis?function=2 (accessed on 9 November 2022) [36,37]

2.3. miRanda

The miRanda algorithm, released in 2003, includes features for analyzing sequence complementarity, seed-based interaction, and miRNA–mRNA duplex dimerization and was released in 2003 [31]. Cross-species target conservation is a key feature of this algorithm for making the prediction. This widely used standard scanning computational algorithm was implemented to predict the miRNA binding sites in the corresponding target region based on the thermodynamic free energy of duplexes [32]. The miRanda algorithm was written in the C programming language. The default parameters were used for miRNA target prediction (Table 1).

2.4. RNA22

The RNA22 algorithm uses a pattern-recognition approach that relies on non-seed-based interactions of miRNA–mRNA pairs. A web-based server is used to predict miRNA binding sites in the target sequence [33]. Highly sensitive and significant target patterns were predicted based on maximum folding energy (MFE) [34]. The default parameters were selected for the prediction of multiple target sites (Table 1).

2.5. TAPIR

The TAPIR algorithm is a recently developed web server used to precisely select highly specific miRNA–mRNA duplexes. TAPIR is also known as Tapirhybrid. The algorithm has been widely used to identify seed-based miRNA target binding sites based on the minimum free energy ratio in plants [35]. Target prediction was performed using the standard (default) parameters (Table 1).

2.6. *psRNATarget*

The *psRNATarget* algorithm is based on the highly sensitive recognition of cleavage patterns and uses a complementarity assessment scheme for predicting multiple binding sites of plant miRNAs in the target sequences and is available on a web server [36,37]. The published 207 apple *mdm*-miRNAs were selected in the web server for analysis. Standard parameters were chosen for the prediction of multiple target sites (Table 1).

2.7. *Discovering Apple mdm-miRNA-Target Interactions*

The apple mature *mdm*-miRNAs and target ORFs of ACLSV were plotted using the Circos algorithm [38].

2.8. *RNAfold*

The *RNAfold* algorithm is available on a web server implemented in the ViennaRNA package [39]. It is used to construct the secondary structures of consensus *mdm*-miRNA precursors. The precursor sequences of apple *mdm*-miRNAs were analyzed using the default settings.

2.9. *RNAcofold*

The *RNAcofold* algorithm evaluates miRNA–mRNA interactions by estimating the free energy (ΔG) of duplexes [40]. The consensus FASTA sequences of the mature apple *mdm*-miRNAs and target sequences of ACLSV were analyzed using the default settings.

2.10. *Statistical Analysis*

The predicted miRNA sequence data are as graphical interpretations. The R language (version 3.1.1) is a widely used tool for interpreting and visualizing biological data [41].

3. Results

3.1. *Apple Genome-Encoded mdm-miRNAs Targeting ACLSV Genome*

The *in silico* approach to identifying apple *mdm*-miRNAs with predicted potential to target the ACLSV +ssRNA-mRNA among the 322 locus-derived *mdm*-miRNAs in the apple genome, was investigated using a predictive approach involving “four algorithms”. The miRanda algorithm predicted the binding of 37 mature apple *mdm*-miRNAs to 46 target sites in the ACLSV genome. The RNA22 algorithm predicted 108 *mdm*-miRNAs targeting 161 ACLSV genome sites. The TAPIR algorithm identified 103 apple genome-encoded *mdm*-miRNA-target pairs. Finally, the *psRNATarget* identified 109 *mdm*-miRNAs targeting 166 ACLSV genome sites as highly significant “cleavable targets” (Figure 1) (Tables S2 and S3 and File S1).

3.2. *Apple mdm-miRNAs Targeting ORF1 That Encodes Replication-Associated Protein*

The trichoviral ORF1 (140–5773) (5634 bases) encodes the replication-associated polyprotein (Rep) that harbors the RNA-dependent RNA polymerase (RdRp), essential for genome replication [42,43]. The miRanda algorithm predicted the binding of thirty one apple *mdm*-miRNAs: *mdm*-miR159c (start site 4379), *mdm*-miR160 (a, b, c, d, e) (4197), *mdm*-miR169a (4217, 3355), *mdm*-miR169 (e, f) (1571), *mdm*-miR169 (g, h, i, and j) (4217,3355), *mdm*-miR393 (g, h) (3091), *mdm*-miR395k (4691), *mdm*-miR3627d (2376), *mdm*-miR5225 (a, b) (182), *mdm*-miR5225c (4719), *mdm*-miR7121 (a, b, c, d, e, f, g, and h) (149), *mdm*-miR10998 (3899), and *mdm*-miR11012 (a, b) (4585) (Figure 2A).

The RNA22 predicted eighty-two apple *mdm*-miRNAs: *mdm*-miR160 (start site a, b, c, d, e) (2133, 4424), *mdm*-miR166f (963, 4194), *mdm*-miR167a (975), *mdm*-miR167 (b, c, d, e, f, g, h, i, and j) (3231), *mdm*-miR168 (a, b) (2504, 3030), *mdm*-miR169o (345), *mdm*-miR171f-3p (3230), *mdm*-miR171f-5p (5101), *mdm*-miR171o (836), *mdm*-miR171q (5101), *mdm*-miR172 (m, n) (3230), *mdm*-miR319 (a b-3p (5195), *mdm*-miR319c-5p (952, 1743, 3236), *mdm*-miR319h (952, 1743, 3236), *mdm*-miR393 (d, e, f, g, h) (3092), *mdm*-miR394 (a, b)(2587), *mdm*-miR395 (d-5p, g-5p, h, i-5p, and j) (5181), *mdm*-miR395k (4691), *mdm*-miR395l (5592),

mdm-miR408a (2376), mdm-miR477 (a, b) (3659), mdm-miR482a-3p (2135), mdm-miR530 (a, b, c) (4683), mdm-miR535 (a, d) (1652), mdm-miR3627d (2376, 3541), mdm-miR5225 (a, b) (1364) mdm-miR5225c (1718), mdm-miR7121 (a, b, c) (153, 961, 2574), mdm-miR7121 (d, e, f, g, h) (2574, 4538), mdm-miR10978 (a, b) (1644), mdm-miR10979 (2150), mdm-miR10980 (a, b) (2630, 4198), mdm-miR10983 (5399), mdm-miR10984b-3p(2584), mdm-miR10993 (c, d, e, f) (972), mdm-miR10994-3p (2217), mdm-miR10995 (960, 4695), mdm-miR10996a (3100), mdm-miR11002 (a, b, c-3p) (558, 4139, 5331), mdm-miR11012 (a, b) (4582), and mdm-miR11019 (964) (Figure 2B).

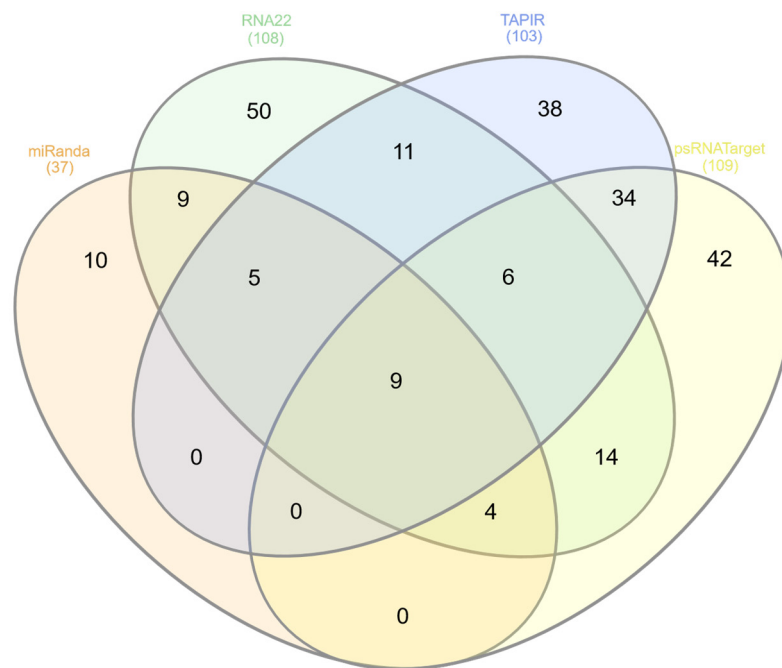


Figure 1. Venn diagram showing common and exclusive locus-derived mdm-miRNAs in the apple genome predicted to interact with ACLSV +ssRNA-encoded mRNAs. In this study, four algorithms (namely miRanda, RNA22, TAPIR, and psRNATarget) were implemented to identify the most effective, predicted apple mdm-miRNA-binding sites in the ACLSV genome. The overlapping sequence identified by the collective algorithms in the in silico toolbox reflect the binding site level. The intersection of four tools in this Venn plot yielded nine unique apple mdm-miRNAs.

The TAPIR algorithm identified multiple mdm-miRNAs: mdm-miR167a (start site 976), mdm-miR168 (a, b) (2505), mdm-miR169 (k, l, m, n, o) (200), mdm-miR171 (m, n) (700), mdm-miR319 (b-5p, d, e, f) (5373), mdm-miR390 (a, b, c, d, e, f) (687), mdm-miR393 (d, e, f) (3091), mdm-miR394a (1426), mdm-miR394b (1970), mdm-miR395 (a, b, c, d-3p, e, f, g-3p, h, and i-3p,) (1970), mdm-miR395k (4691), mdm-miR396 (a, c, d, e) (2702), mdm-miR397 (a, b) (3331), mdm-miR399 (e, f, g, h) (1443), mdm-miR403 (a, b) (2053), mdm-miR477a (2028), mdm-miR482a-3p (2136), mdm-miR482b (2207), mdm-miR530 (a, b, c) (4730), mdm-miR5225c (4490), mdm-miR7120 (a-3p, b-3p) (2867), mdm-miR7121 (a, b, c, d, e, f, g, and h) (1755), mdm-miR10981 (c, d) (5024), mdm-miR10983 (3324), mdm-miR10986 (5404), mdm-miR10989 (a, b, c, d, e) (3173), and mdm-miR10991(a, b, c, d, e) (4997) (Figure 2C and Tables S2 and S3).

Several “potentially efficient” locus-derived mdm-miRNAs occurring in the apple genome were predicted by the psRNATarget algorithm: mdm-miR156 (ad, ae) (2674), mdm-miR159 (a, b) (375), mdm-miR164 (b, c, d, e, f) (2670), mdm-miR166 (a, b, c, d, e, f, g, h, and i) (781), mdm-miR169 (e, f) (2669), mdm-miR171o (581), mdm-miR172 (a, b, c, d, e, f, g, h, I, j, k, l, m, n, o) (5580), mdm-miR319 (a, b) (2232), mdm-miR394 (a, b) (1426, 4195), mdm-miR395 (a, b, c, d, e, f, g, h, and i) (1970, 4121), mdm-miR396 (a, b, c, d, e, f, g) (2702, 3376), mdm-miR399 (e, f, g, h) (1443), mdm-miR408 (a) (2218, 1410), mdm-miR408 (b, c,

d) (2668), mdm-miR482a-5p (4111), mdm-miR535 (a, d) (1652), mdm-miR858 (4465, 4296), mdm-miR2111 (a, b) (1021, 4893), mdm-miR5225 (a, b) (1340, 5233), mdm-miR5225c (266, 4490), mdm-miR7120 (a, b) (5128, 4556, 3088), mdm-miR7121(a, b, c, d, e, f, g, and h) (1755), mdm-miR7123 (a, b) (1567), mdm-miR7125 (5489), and mdm-miR7126 (1910) (Figure 2D) (Tables S2 and S3).

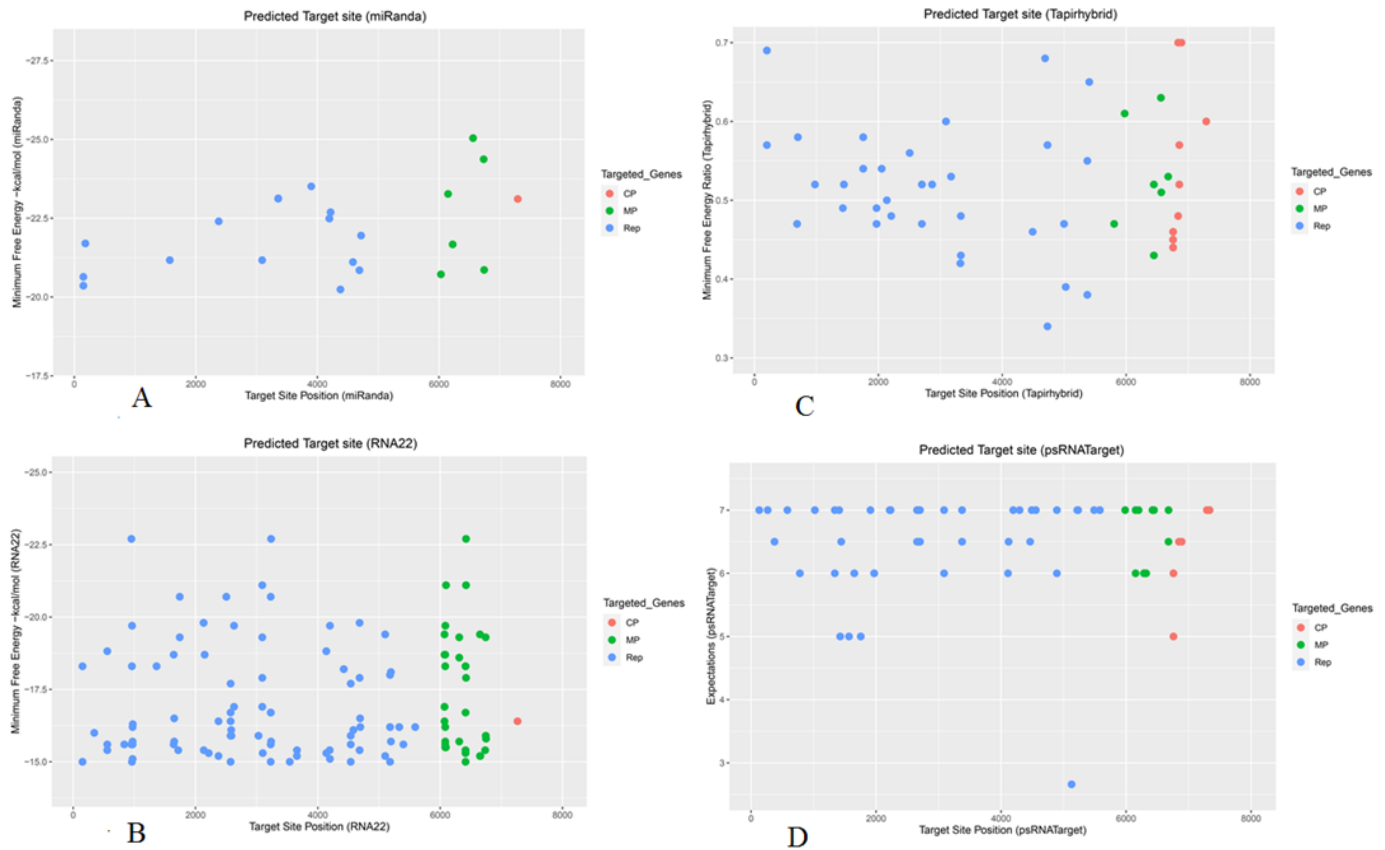


Figure 2. Predictions of mature apple mdm-miRNA target sites in the ACLSV genome were obtained using the following in silico algorithms: (A) miRanda; (B) RNA22; (C) TAPIR or Tapirhybrid; (D) psRNATarget. Each colored dot shows a single binding site of the predicted mdm-miRNA in the ACLSV genome. The ORFs encoded on the ACLSV genome are represented by a different color.

3.3. Apple mdm-miRNAs Targeting ORF2 That Encodes Movement Protein

The ACLSV ORF2 (5685–7067) (1382 nucleotides) encodes a multifunctional movement protein (MP) required for cell-to-cell movement of ACLSV [44–47]. The miRanda algorithm predicted several apple mdm-miRNAs putatively capable of silencing the movement protein by targeting ORF2: mdm-miR319d (start site 6744), mdm-miR828 (a, b) (6033), mdm-miR3627d (6736), mdm-miR5225 (a, b) (6226), mdm-miR10980 (a, b) (6561), and mdm-miR11008 (6150) (Figure 2A).

The RNA22 predicted binding of potential apple mdm-miRNAs to target ORF2: mdm-miR164 (a, b, c, d, e, f) (start site 6096), mdm-miR169 (e, f) (6750), mdm-miR171(a, b) (6071), mdm-miR171f-5p (6651), mdm-miR171 (j, k, l, p) (6071), mdm-miR171 (q) (6071, 5101), mdm-miR319d (6744), mdm-miR393 (d, e, f)(6423), mdm-miR394 (a, b) (6746), mdm-miR399 (a, b, c, d, i, j) (6083), mdm-miR482a-5p (6657), mdm-miR530 (a, b, c) (6312), mdm-miR3627d(6736), mdm-miR7121 (a, b, c, d, e, f, g, h) (6415), and mdm-miR10981 (a, b) (6085) (Figure 2B).

The TAPIR algorithm predicted eight mdm-miRNAs: mdm-miR169b (6678), mdm-miR396 (e, f) (6447), mdm-miR3627d (6567), mdm-miR7125 (5806), mdm-miR10980 (a, b) (6561), mdm-miR10994-3p (5976) (Figure 2C). Several potential apple mdm-miRNAs were predicted by the psRNATarget algorithms: mdm-miR169 (b, c, d) (6678), mdm-miR171o

(5985), mdm-miR390 (a, b, c, d, e, f) (6321), mdm-miR393 (d, e, f) (6432), mdm-miR395 (a, b, c, d, e, f, g, h, i) (6286), mdm-miR396 (f, g) (6447), mdm-miR397 (a, b) (6152), mdm-miR482b (6432), and mdm-miR5225c (6200) (Figure 2D) (Tables S2 and S3).

3.4. Apple mdm-miRNAs Targeting ORF3 That Encodes Coat Protein

The ACLSV ORF3 (6751–7332 bp) (581 nucleotides) encodes a capsid protein (CP) involved in encapsidation of trichoviral ssRNA into a virion, or particle [48,49]. A single mdm-miRNA (mdm-miR5225c) was identified that was located at nucleotide position 7297 by the miRanda algorithm (Figure 2A). Two unique apple mdm-miRNAs were identified by RNA22: mdm-miR168 (a, b) (7265) (Figure 2B).

Several potential apple mdm-miRNAs were predicted to target ORF3 for silencing the coat protein gene by the TAPIR algorithm: mdm-miR156 (p, q, r, s, x, y, z) (6758), mdm-miR156 (aa, ab, ac, ad, ae) (6758, 7293), mdm-miR397b (6839), mdm-miR398 (b, c) (6839), mdm-miR11001 (6858), mdm-miR11016 (6858) (Figure 2C). In addition, nineteen mdm-miRNAs were predicted with psRNATarget: mdm-miR156 (p, q, r, s) (6758), mdm-miR156 (ab, ac, ad, ae) (6758, 7293), mdm-miR166 (a, b, c, d, e, f, g, h, i) (7335), mdm-miR398a (6890), and mdm-miR858 (6846) (Figures 2D and 3) (Tables S2 and S3).



Figure 3. Union plot indicating the entire set of predicted apple mdm-miRNA binding sites for the ACLSV genome. This plot is created as a union by all tools. The y axis shows the minimum free energy (MFE) in the range of -0 – 30 Kcal/mol for miRanda and RNA22 analysis, the MFE ratio (range 0 – 1) for TAPIR, and also the expected value in the range of 0 – 10 for psRNATarget. The x-axis represents the genomic position in the range of 1 – 7545 nucleotides.

3.5. Evaluation of Common Apple MicroRNAs

Based on the predicted locus-derived mdm-miRNAs in the apple genome, nine miRNAs (mdm-miR5225c and mdm-miR7121 (a, b, c, d, e, f, g, and h)) were detected as having potential binding sites in the ACLSV genome when considering the consensus from all four algorithms (Figures 1 and 3).

3.6. Evaluation and Identification of Consensual Apple MicroRNAs for ACLSV Silencing

Using a combination of the “four algorithms miRanda, RNA22, TAPIR, and psRNA-Target, the consensus is expected to yield high accuracy and robustness for identifying locus-derived mdm-miRNAs in the apple genome that may potentially interact with the viral genome. The consensus for the genomic binding sites was predicted using the tools described, to analyze the biological data available in the public databases.

Of the 322 targeting mature apple tree mdm-miRNAs, 58 apple mdm-miRNAs (mdm-miR156 (start site o, p, q, r, ab, ac) at nucleotide (nt) position 6758, mdm-miR156 (ad, ae) at nt position 7293, mdm-miR167a at nt position 976, mdm-miR168 (a, b) at nt position 2505, mdm-miR169b at nt position 6678, mdm-miR319d at nt position 6744, mdm-miR393 (d, e, f, g, h) at nt position 3092, mdm-miR393 (d, e, f) at nt position, mdm-miR394a at nt position 1426, mdm-miR395 (a, b, c, d, e, f, g, h, i) at nt position 1970, mdm-miR395k at nt positions 4691, mdm-miR396 (a, c, d, e) at nt position 2702, mdm-miR396 (f, g) at nt position 6447, mdm-miR399 (e, f, g, h) at nt position 1443, mdm-miR482a-3p at nt position 2136, mdm-miR535(a, d) at nt position 1652, mdm-miR3627d at nt positions 2376 and 6736, mdm-miR5225c at nt position 4490, mdm-miR7121 (a, b, c, d, e, f, g, h) at nt positions 153 and 1755, mdm-miR10980 (a, b) at nt position 6561, and mdm-miR11012 (a, b) at nt position 4585) were detected based on the consensus of the two algorithms (Figure 4, Table 2, Tables S2 and S3).

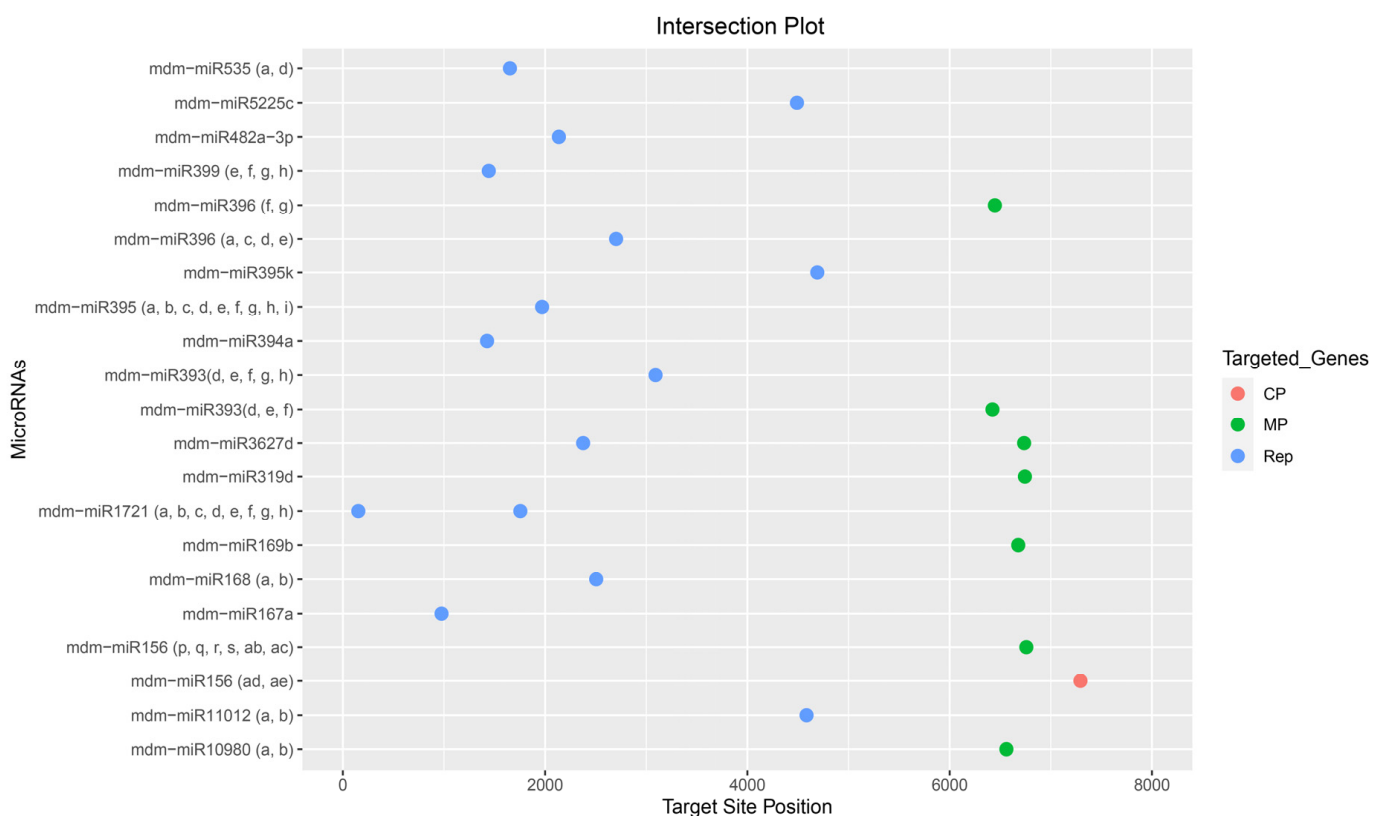


Figure 4. The intersection plot shows the consensus apple mdm-miRNAs targeting the ACLSV genome. The predicted mdm-miRNA binding sites were based on the consensus or combined results of both algorithms.

Based on the identification of 58 consensus mdm-miRNAs, nine apple tree mdm-miRNAs, mdm-miR7121 (a, b, c, d, e, f, g, h) (start site 1755) (target protein Rep), and mdm-miR395k (4691) (Rep) were predicted to be the most effective mdm-miRNAs for targeting the ACLSV genome (Figure 4).

Table 2. Target binding sites of consensus apple genome-encoded mdm-miRNAs, determined by combined results of two algorithms.

Apple miRNAs	Position miRanda	Position RNA22	Position TAPIR	Position psRNATarget	MFE * miRanda	MFE ** RNA22	MFE Ratio TAPIR	Expectation psRNATarget
mdm-miR156 (p, q, r, s)			6758	6758			0.44	6.00
mdm-miR156 (ab, ac)			6758	6758			0.46	5.00
mdm-156 (ad, ae)			7293	7293			0.60	7.00
mes-miR167a			975	976		−16.30	0.52	
mdm-miR168 (a, b)		2504	2505			−20.70	0.56	
mdm-miR169b			6678	6678			0.53	6.50
mdm-miR319d	6744	6744			−20.86	−18.10		
mdm-miR393 (d, e, f)		6423		6423		−19.30		7.00
mdm-miR393 (d, e, f)		3092	3091			−22.70	0.60	
mdm-miR393 (g, h)	3091	3092			−21.17	−21.11		
mdm-miR394 (a, b)			1426	1426			0.49	5.00
mdm-miR395 (a, b, c, d, e, f, g, h, i)			1970	1970			0.47	6.00
mdm-miR395k	4691	4691	4691		−20.85	−18.00	0.68	
mdm-miR396 (a, c, d, e)			2702	2702			0.52	6.50
mdm-miR396 (f, g)			6447	6447			0.43	7.00
mdm-399 (e, f, g, h)			1443	1443			0.52	6.50
mdm-482a-3p		2135	2136			−18.30	0.48	
mdm-482b			2207				0.34	6.00
mdm-535a		1652	1652			−18.60		6.00
mdm-535b		1652	1652			−17.90		6.50
mdm-miR3627d	2376	2376			−22.40	−19.30		
mdm-miR3627d (1)	6736	6736			−24.37	−19.80		
mdm-5225c			4490	4490			0.46	7.00
mdm-7121 (a, b, c)	149	153	1755	1755	−20.63	−22.40	0.58	5.00
mdm-miR7121 (d, e, f, g, h)			1755	1755			0.58	5.00
mdm-miR10980 (a, b)	6561		6561		−25.04		0.63	
mdm-miR11012 (a, b)	4585	4582			−21.11	−18.82		

* MFE is an abbreviation of minimum free energy. MFE ** is the maximum folding energy.

3.7. Construction of Apple mdm-miRNAs-mRNA Regulatory Network

Validation of the predicted interaction between host miRNAs and ACLSV genome was visualized and created by a “Circos map”. The predicted Circos map shows a comprehensive global view of the integrated apple mdm-miRNAs and the corresponding target genes of the ACLSV genome. A Circos plot was drawn to enable a comprehensive visualization of genomic data that reduces graph complexity and improves readability.

The interaction data were visualized as a chord diagram connecting the corresponding apple locus-derived mdm-miRNAs and ORFs of the ACLSV genome (Figure 5). Biological data were analyzed to generate the chord diagram (Circos plot) using R software. It supports using the grammar of graphics syntax to present data as follows: Library (circlize), chordDiagram (data, grid.col = “white”, annotation Track = “grid”).

3.8. Secondary Structures of the Consensual RNA

The in silico identification, prediction, and validation of the consensus apple genome-encoded mdm-miRNAs (mdm-MIR5225c, mdm-MIR395k, and mdm-MIR7121 (a, b, c, d, e, f, g, h)) were selected based on the predicted secondary structure of the pre-miRNA sequences (Figure 6 and Table 3).

The adjusted minimal folding free energy (AMFE) was estimated using $AMFE = (MFE/\text{length of a potential pre-miRNA}) \times 100$. The minimal folding free energy index (MFEI) was calculated $(MFEI = ((100 \times MFE)/\text{Length of RNA}/(G + C))\%)$, based on the previously reported equation [50]. The higher AU content depicts a comparatively less stable pre-miRNA secondary structure that would be readily recognized by the RISC complex and converted into mature miRNA. The minimal folding free energy (MFE) is considered an important determining factor that reflects the stability of the secondary structure. The lower the MFE value, the higher the thermodynamic stability of the secondary structure [51].

3.9. Assessment of Free Energy

Evaluation and validation of the consensus locus-derived mdm-miRNAs in the apple genome was determined by assessing their duplex binding free energies (ΔG) (Table 4). The implementation of free energy evaluation further helps to screen the most reasonable candidates for genome silencing of ACLSV. An acceptable amiRNA–target duplex must

have at least 70% of the free hybridization energy calculated for a perfectly complementary amiRNA [52]. The RNAfold algorithm was used to analyze the secondary structure of the common miRNA binding site, and the Vienna RNAfold prediction is based on the minimum free energy model [53].

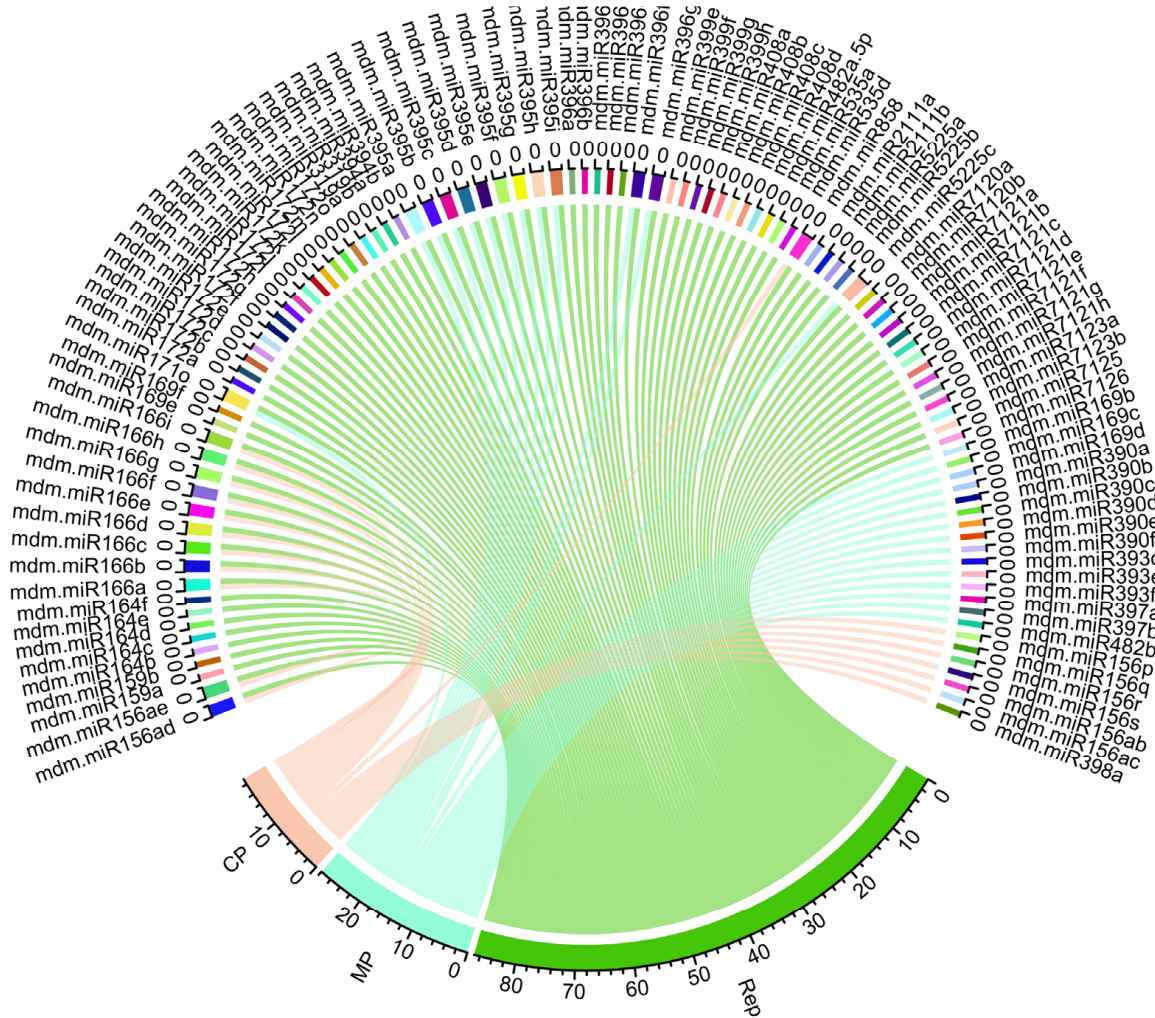


Figure 5. An integrated interaction map of locus-derived mdm-miRNAs in the apple genome and ACLSV ORFs, viral-ORFs indicated as colored lines.

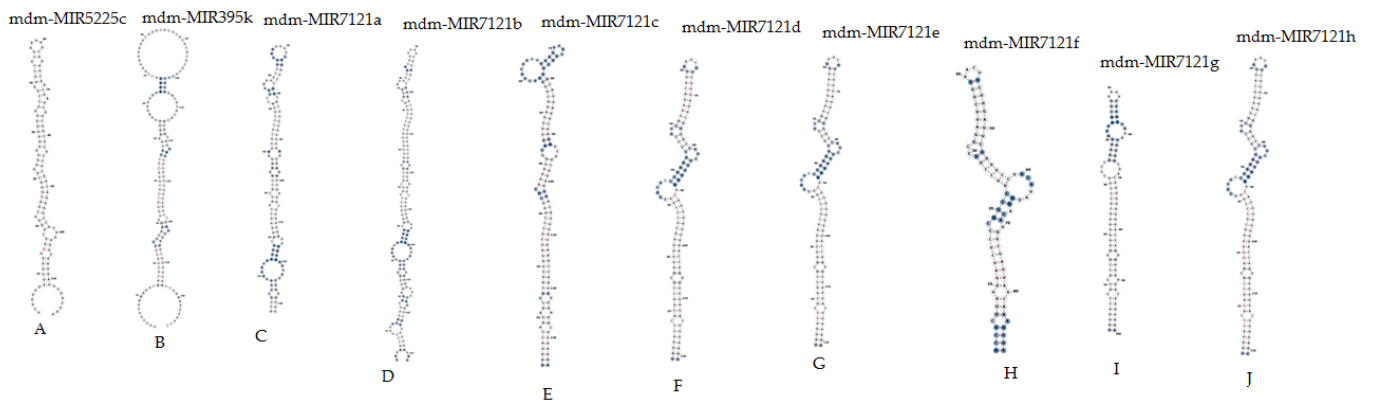


Figure 6. Prediction of stable secondary structures of the ACLSV precursors. Ten pre-miRNA secondary structures were determined.

Table 3. Characterization and salient features of the consensus precursors of locus-derived mdm-miRNAs in the apple genome analyzed in this study.

miRNA ID	Accession IDs	Length Precursor	MFE/Kcal/mol	AMFE	MFEI	(G + C)%
mdm-MIR5225c	MI0023156	119 nt	−51.30	−43.10	−0.85	50.42
mdm-MIR395k	MI0035639	168 nt	−43.27	−25.75	−0.68	37.50
mdm-MIR7121a	MI0023144	132 nt	−49.40	−37.42	−0.79	46.97
mdm-MIR7121b	MI0023145	172 nt	−70.60	−41.04	−0.85	48.26
mdm-MIR7121c	MI0023146	135 nt	−71.30	−52.81	−1.09	48.15
mdm-MIR7121d	MI0023147	121 nt	−67.50	−55.78	−1.08	51.24
mdm-MIR7121e	MI0023148	121 nt	−67.50	−55.78	−1.08	51.24
mdm-MIR7121f	MI0023149	88 nt	−39.90	−45.34	−0.79	56.82
mdm-MIR7121g	MI0023150	100 nt	−45.80	−45.80	−0.89	51.00
mdm-MIR7121h	MI0023151	121 nt	−67.50	−55.78	−1.08	51.24

Table 4. Free energy (ΔG) post-apple plant mdm-miRNA–mRNA duplex formation.

Apple Mature miRNA ID	Accession ID	Mdm-miRNA-Target Sequence (5'–3')	ΔG Duplex (Kcal/mol)
mdm-miR5225c	MIMAT0026052	5' UCUGUCGUGGGUGAGAUGGUGC 3' 5' GAAGCAGTGTACCCAAGACATA 3'	−15.90
mdm-miR395k	MIMAT0043586	5' GUUCCUCAAAACACUUCUU 3' 5' AGGCAGGAGTTTGAGGAAAC 3'	−18.30
mdm-miR7121a	MIMAT0026040	5' UCCUCUUGGUGAUCGCCUGU 3' 5' AAAGGGAGTTCATCGAGAGAA 3'	−22.10
mdm-miR7121b	MIMAT0026041	5' UCCUCUUGGUGAUCGCCUGU 3' 5' AAAGGGAGTTCATCGAGAGAA 3'	−22.10
mdm-miR7121c	MIMAT0026042	5' UCCUCUUGGUGAUCGCCUGU 3' 5' AAAGGGAGTTCATCGAGAGAA 3'	−22.10
mdm-miR7121d	MIMAT0026043	5' UCCUCUUGGUGAUCGCCUGC 3' 5' AAAGGGAGTTCATCGAGAGAA 3'	−22.10
mdm-miR7121e	MIMAT0026044	5' UCCUCUUGGUGAUCGCCUGC 3' 5' AAAGGGAGTTCATCGAGAGAA 3'	−22.10
mdm-miR7121f	MIMAT0026045	5' UCCUCUUGGUGAUCGCCUGC 3' 5' AAAGGGAGTTCATCGAGAGAA 3'	−22.10
mdm-miR7121g	MIMAT0026046	5' UCCUCUUGGUGAUCGCCUGC 3' 5' AAAGGGAGTTCATCGAGAGAA 3'	−22.10
mdm-miR7121h	MIMAT0026047	5' UCCUCUUGGUGAUCGCCUGC 3' 5' AAAGGGAGTTCATCGAGAGAA 3'	−22.10

4. Discussion

The ACLSV belongs to the genus *Trichovirus*, and infected trees exhibit reduced vigor and yield. The ACLSV has been identified infecting fruit trees in numerous countries in the last three decades. The discovery that amiRNA may be among the best option for combating plant virus diseases has led to extensive research in the plant biotechnology arena [54]. Several studies have demonstrated the expression of endogenous plant miRNAs that can directly target RNA or DNA viruses based on a predictive approach that implements “four algorithms” to arrive at consensus solutions [55–61]. Recent studies have shown that expression of amiRNA-based constructs in economically important transgenic crops can reduce or eliminate the viral load in infected plants, resulting from infection by both RNA and DNA viruses [22,23,62–67]. Until now, the potential for exploiting the regulation of apple genome-encoded miRNA to abate infection of apple trees by ACLSV has not been investigated as strategy for developing tolerant or resistant apple cultivars. The results of this study provide the first computationally-based evaluation of mature locus-derived mdm-miRNAs in the apple plant genome to enable prediction of effective miRNA-binding sites and provide new tools for better understanding the molecular and omic interactions between apple plant host cells and ACLSV-encoded mRNAs/protein.

In silico algorithms have been widely used to predict miRNA-binding sites in the target region to study host–virus interactions [68]. The use of computational biology and machine learning approaches, that enable highly accurate prediction of optimal target regions in viral genomes with low rates of false-positive predictions is key to accurately identifying

potential miRNA-mRNA interactions. Here, four algorithm-based approaches, miRanda, RNA22, TAPIR, and psRNATarget, were used to predict and analyze potential apple plant-mdm-miRNA-mRNA interactions with ACLSV. Several potential apple miRNA binding sites involved in miRNA-mRNA interactions were consistently identified by all four algorithms implemented in this study. The miRanda and TAPIR algorithms were found to be powerful multimorbidity algorithms that identify seed-based interactions in the target region. The miRanda algorithm is a web-based algorithm and the most widely used miRNA binding site predictor based on a dynamic programming algorithm and a thermodynamic MFE calculation.

The miRanda, RNA22, and TAPIR algorithms identified a consensus binding site of mdm-miR395k at nucleotide position 4691. The apple common mdm-miR5225c and mdm-miR7121 (a, b, c, d, e, f, g, h) were the most potent predicted miRNAs based on the collective results obtained when data resulting from all four algorithms were considered (Figure 4 and Table 2). The TAPIR and psRNATarget algorithms were used to predict the binding strength of mdm-miR5225c and mdm-miR7121 (a, b, c, d, e, f, g, h) at consensus viral genome positions, 4490 and 1755, respectively.

To predict miRNA binding sites of the target sequence based on MFE which is also interpreted for evolutionary inference [69]. The stability of miRNA-mRNA duplex is related to binding energy. Functional miRNA target recognition depends on the accessibility of the binding site, which is a key feature of in silico algorithms for evaluating false-positive miRNA-target interactions. The validation of miRNA-target interactions also depends on the MFE [70]. A high probability of miRNA-target interaction was set to a lower value of MFE [71]. The highest stability of miRNA-mRNA duplex is realized based on achieving the most robust binding affinity of miRNA to target mRNA [72,73]. The prediction, evaluation, and validation of miRNA targeting patterns were based on base-pairing probability of mdm-miRNA seed regions with complementary high-affinity binding sites, within the ACLSV genome. The MFE of mdm-miR395k was calculated to be -20.85 kcal/mol (miRanda), -18.00 kcal/mol (RNA22) (Table 2), and -18.30 kcal/mol (RNAcofold) (Table 4), support the predicted results, which are indicative of high stability of miRNA-mRNA duplexes representing “true targets”.

When used with a free energy assessment, the approach provided apparently highly reliable predictions of miRNA target binding sites and resulted in identification of ten consensus potent apple miRNAs (Tables 2–4). These predicted apple mdm-miRNAs have robust potential for RNAi-based gene silencing. Future work will focus on amiRNA-based constructs directed toward silencing the ACLSV genome for transformation of desirable apple cultivars.

Computational analyses revealed that the apple consensus mdm-miR395k is expected to target ACLSV ORF1 sequences. The apple precursor mdm-MIR395k (NCBI Accession ID: MI0035639) was located on apple chromosome MDC003846.250 (genome context coordinates 8270 to 8437) [74]. In apple, Md-miR395 was shown to control the transcription factor *MdWRKY26* to regulate resistance to leaf spot disease [24]. The miR395 is involved in the regulation of carbohydrate accumulation gene (NADP-MDH) for flower development in camellia plants [75]. Our studies show that locus-derived mdm-miRNAs in the apple genome directly pair with specific sites on ACLSV +ssRNA-encoded mRNAs. In the current study, we developed a model to estimate the prediction probability using different approaches to reduce false positives at the individual, consensus, and intersection levels. The union approach is a highly sensitive approach for miRNA candidate prediction based on the combination of more than one miRNA prediction tool. To increase the specificity of the predictions, an intersection approach was implemented that is based entirely on prediction specificity [76]. The apparently highly reliable target predictions suggest that the in silico strategy implemented has yielded “high efficiency” predictions at the individual, union, and intersection levels, and identified the best target binding sites of the studied apple mdm-miRNAs (Figures 1–4 and Table 2).

While previous studies have focused primarily on sequencing of full-length ACLSV genome [10,11,77,78], in this study, locus-derived mdm-miRNAs were identified from the apple genome that directly bind to multiple consensus genomic regions of ACLSV. Further, no previous report has shown that apple mdm-miRNAs bind to ACLSV, predicting several, functionally related, host-miRNA–virus-mRNA interactions. It is further anticipated that the sequences predicted herein will be valuable for studying the mechanisms involved in host-virus interactions at the biological, genetic, and omic levels. While this study has evaluated the in silico interactions between apple genome-encoded mdm-miRNAs and ACLSV, whether the predicted apple mdm-miRNAs can bind to ACLSV sequences remains to be investigated. Definitive experiments are also needed to determine the binding strength of the predicted mdm-miRNAs in transgenic apple plants.

5. Conclusions and Future Directions

The ACLSV has emerged as a damaging pathogen to pome and stone fruit trees worldwide. This study involves the comprehensive and computational characterization of mdm-miRNAs encoded in apple plants, predicted to feasibly silence ACLSV. Potential apple mdm-miRNA candidates targeting ACLSV were screened using four “algorithms”. Among the 322 apple mdm-miRNAs from the miRBase database, only one mdm-miRNA (mdm-miR395k) was predicted to be impede ACLSV replication by targeting the genomic consensus position, start site 4691, to silence the ACLSV Rep protein. This approach offers specificity and sensitivity and complements existing molecular approaches for analyzing targets for ACLSV disease abatement. Results indicate that the use of in silico tools provides better results than a single algorithm when developing amiRNA-based mdm-miRNA therapeutics to target ACLSV and other plant viruses as well.

Supplementary Materials: The following supporting information can be downloaded at: <https://www.mdpi.com/article/10.3390/horticulturae9070808/s1>, Table S1: Mature mdm-miRNAs of apple tree; Table S2: Identification of mdm-miRNA binding sites of apple using multiple algorithms; Table S3: Gene-wise prediction of mdm-miRNA-binding sites; File S1: Prediction results by different computational tools.

Author Contributions: M.A.A., J.K.B. and N.Y. conceived the original idea for this work. All the authors performed, analyzed, and interpreted the in silico data. M.A.A. and N.M. wrote the manuscript. J.K.B. edited the manuscript and wrote the abstract and discussion. All authors have read and agreed to the published version of the manuscript.

Funding: This research was funded by Central Public-interest Scientific Institution Basal Research Fund (1630052023003). The research work was completed under a MoU among the three institutes mentioned.

Institutional Review Board Statement: Not applicable.

Informed Consent Statement: Not applicable.

Data Availability Statement: Not applicable.

Conflicts of Interest: The authors declare no conflict of interest.

References

1. Na, W.; Wolf, J.; Zhang, F.-S. Towards sustainable intensification of apple production in China—Yield gaps and nutrient use efficiency in apple farming systems. *J. Integr. Agric.* **2016**, *15*, 716–725.
2. Shah, Z.A.; Dar, M.A.; Dar, E.A.; Obianefo, C.A.; Bhat, A.H.; Ali, M.T.; El-Sharnouby, M.; Shukry, M.; Kesba, H.; Sayed, S. Sustainable Fruit Growing: An Analysis of Differences in Apple Productivity in the Indian State of Jammu and Kashmir. *Sustainability* **2022**, *14*, 14544. [[CrossRef](#)]
3. Chen, Z.; Yu, L.; Liu, W.; Zhang, J.; Wang, N.; Chen, X. Research progress of fruit color development in apple (*Malus domestica* Borkh.). *Plant Physiol. Biochem.* **2021**, *162*, 267–279. [[CrossRef](#)] [[PubMed](#)]
4. Velasco, R.; Zharkikh, A.; Affourtit, J.; Dhingra, A.; Cestaro, A.; Kalyanaraman, A.; Fontana, P.; Bhatnagar, S.K.; Troggio, M.; Pruss, D. The genome of the domesticated apple (*Malus × domestica* Borkh.). *Nat. Genet.* **2010**, *42*, 833–839. [[CrossRef](#)]
5. Martelli, G.; Candresse, T.; Namba, S. *Trichovirus, a New Genus of Plant Viruses*; Springer: Berlin/Heidelberg, Germany, 1994.

6. Rwahni, M.A.; Turturo, C.; Minafra, A.; Saldarelli, P.; Myrta, A.; Pallás, V.; Savino, V. Molecular variability of apple chlorotic leaf spot virus in different hosts and geographical regions. *J. Plant Pathol.* **2004**, *86*, 117–122.
7. Abtahi, F.; Shams-Bakhsh, M.; Safaie, N.; Azizi, A.; Autonell, C.R.; Ratti, C. Incidence and genetic diversity of apple chlorotic leaf spot virus in Iran. *J. Plant Pathol.* **2019**, *101*, 513–519. [[CrossRef](#)]
8. Katsiani, A.; Maliogka, V.; Candresse, T.; Katis, N. Host-range studies, genetic diversity and evolutionary relationships of ACLSV isolates from ornamental, wild and cultivated Rosaceous species. *Plant Pathol.* **2014**, *63*, 63–71. [[CrossRef](#)]
9. Yaegashi, H.; Yoshikawa, N.; Candresse, T. Apple chlorotic leaf spot virus in pome fruits. In *Virus and Virus-Like Diseases of Pome and Stone Fruits*; Hadidi, A., Barba, M., Candresse, T., Jelkmann, W., Eds.; APS Press/American Phytopathological Society: St. Paul, MN, USA, 2011; pp. 17–21.
10. Guo, W.; Zheng, W.; Wang, M.; Li, X.; Ma, Y.; Dai, H. Genome sequences of three apple chlorotic leaf spot virus isolates from hawthorns in China. *PLoS ONE* **2016**, *11*, e0161099. [[CrossRef](#)]
11. Canales, C.; Morán, F.; Olmos, A.; Ruiz-García, A.B. First detection and molecular characterization of Apple stem grooving virus, apple chlorotic leaf spot virus, and apple hammerhead viroid in loquat in Spain. *Plants* **2021**, *10*, 2293. [[CrossRef](#)]
12. Dhir, S.; Zaidi, A.A.; Hallan, V. Molecular Characterization and Recombination Analysis of the Complete Genome of Apple Chlorotic Leaf Spot Virus. *J. Phytopathol.* **2013**, *161*, 704–712. [[CrossRef](#)]
13. Reinhart, B.J.; Weinstein, E.G.; Rhoades, M.W.; Bartel, B.; Bartel, D.P. MicroRNAs in plants. *Genes Dev.* **2002**, *16*, 1616–1626. [[CrossRef](#)] [[PubMed](#)]
14. Liu, W.; Meng, J.; Cui, J.; Luan, Y. Characterization and function of microRNA* s in plants. *Front. Plant Sci.* **2017**, *8*, 2200. [[CrossRef](#)]
15. Kim, Y.J.; Zheng, B.; Yu, Y.; Won, S.Y.; Mo, B.; Chen, X. The role of Mediator in small and long noncoding RNA production in Arabidopsis thaliana. *EMBO J.* **2011**, *30*, 814–822. [[CrossRef](#)] [[PubMed](#)]
16. Fang, X.; Cui, Y.; Li, Y.; Qi, Y. Transcription and processing of primary microRNAs are coupled by Elongator complex in Arabidopsis. *Nat. Plants* **2015**, *1*, 15075. [[CrossRef](#)]
17. Fang, Y.; Spector, D.L. Identification of nuclear dicing bodies containing proteins for microRNA biogenesis in living Arabidopsis plants. *Curr. Biol.* **2007**, *17*, 818–823. [[CrossRef](#)] [[PubMed](#)]
18. Manavella, P.A.; Koenig, D.; Weigel, D. Plant secondary siRNA production determined by microRNA-duplex structure. *Proc. Natl. Acad. Sci. USA* **2012**, *109*, 2461–2466. [[CrossRef](#)]
19. Trobaugh, D.W.; Klimstra, W.B. MicroRNA regulation of RNA virus replication and pathogenesis. *Trends Mol. Med.* **2017**, *23*, 80–93. [[CrossRef](#)]
20. Deng, Z.; Ma, L.; Zhang, P.; Zhu, H. Small RNAs Participate in Plant–Virus Interaction and Their Application in Plant Viral Defense. *Int. J. Mol. Sci.* **2022**, *23*, 696. [[CrossRef](#)]
21. Mengistu, A.A.; Tenkegna, T.A. The role of miRNA in plant–virus interaction: A review. *Mol. Biol. Rep.* **2021**, *48*, 2853–2861. [[CrossRef](#)]
22. Zhou, L.; Yuan, Q.; Ai, X.; Chen, J.; Lu, Y.; Yan, F. Transgenic Rice Plants Expressing Artificial miRNA Targeting the Rice Stripe Virus MP Gene Are Highly Resistant to the Virus. *Biology* **2022**, *11*, 332. [[CrossRef](#)]
23. Miao, S.; Liang, C.; Li, J.; Baker, B.; Luo, L. Polycistronic artificial microRNA-mediated resistance to cucumber green mottle mosaic virus in cucumber. *Int. J. Mol. Sci.* **2021**, *22*, 12237. [[CrossRef](#)] [[PubMed](#)]
24. Zhang, Q.; Li, Y.; Zhang, Y.; Wu, C.; Wang, S.; Hao, L.; Wang, S.; Li, T. Md-miR156ab and Md-miR395 target WRKY transcription factors to influence apple resistance to leaf spot disease. *Front. Plant Sci.* **2017**, *8*, 526. [[CrossRef](#)]
25. Qu, D.; Yan, F.; Meng, R.; Jiang, X.; Yang, H.; Gao, Z.; Dong, Y.; Yang, Y.; Zhao, Z. Identification of microRNAs and their targets associated with fruit-bagging and subsequent sunlight re-exposure in the “Granny Smith” apple exocarp using high-throughput sequencing. *Front. Plant Sci.* **2016**, *7*, 27. [[CrossRef](#)] [[PubMed](#)]
26. Niu, C.; Li, H.; Jiang, L.; Yan, M.; Li, C.; Geng, D.; Xie, Y.; Yan, Y.; Shen, X.; Chen, P. Genome-wide identification of drought-responsive microRNAs in two sets of Malus from interspecific hybrid progenies. *Hortic. Res.* **2019**, *6*, 75. [[CrossRef](#)] [[PubMed](#)]
27. Wang, Y.; Feng, C.; Zhai, Z.; Peng, X.; Wang, Y.; Sun, Y.; Li, J.; Shen, X.; Xiao, Y.; Zhu, S. The apple microR171i-SCARECROW-LIKE PROTEINS26.1 module enhances drought stress tolerance by integrating ascorbic acid metabolism. *Plant Physiol.* **2020**, *184*, 194–211. [[CrossRef](#)] [[PubMed](#)]
28. Tahir, M.M.; Li, S.; Liu, Z.; Fan, L.; Tang, T.; Zhang, X.; Mao, J.; Li, K.; Khan, A.; Shao, Y. Different miRNAs and hormones are involved in PEG-induced inhibition of adventitious root formation in apple. *Sci. Hortic.* **2022**, *303*, 111206. [[CrossRef](#)]
29. Kozomara, A.; Birgaoanu, M.; Griffiths-Jones, S. miRBase: From microRNA sequences to function. *Nucleic Acids Res.* **2019**, *47*, D155–D162. [[CrossRef](#)]
30. Sayers, E.W.; Beck, J.; Bolton, E.E.; Bourexis, D.; Brister, J.R.; Canese, K.; Comeau, D.C.; Funk, K.; Kim, S.; Klimke, W. Database resources of the national center for biotechnology information. *Nucleic Acids Res.* **2021**, *49*, D10. [[CrossRef](#)]
31. Enright, A.; John, B.; Gaul, U.; Tuschl, T.; Sander, C.; Marks, D. MicroRNA targets in Drosophila. *Genome Biol.* **2003**, *4*, 1–27. [[CrossRef](#)]
32. John, B.; Enright, A.J.; Aravin, A.; Tuschl, T.; Sander, C.; Marks, D.S. Human microRNA targets. *PLoS Biol.* **2004**, *2*, e363. [[CrossRef](#)]
33. Miranda, K.C.; Huynh, T.; Tay, Y.; Ang, Y.-S.; Tam, W.-L.; Thomson, A.M.; Lim, B.; Rigoutsos, I. A pattern-based method for the identification of MicroRNA binding sites and their corresponding heteroduplexes. *Cell* **2006**, *126*, 1203–1217. [[CrossRef](#)]

34. Loher, P.; Rigoutsos, I. Interactive exploration of RNA22 microRNA target predictions. *Bioinformatics* **2012**, *28*, 3322–3323. [[CrossRef](#)] [[PubMed](#)]
35. Bonnet, E.; He, Y.; Billiau, K.; Van de Peer, Y. TAPIR, a web server for the prediction of plant microRNA targets, including target mimics. *Bioinformatics* **2010**, *26*, 1566–1568. [[CrossRef](#)] [[PubMed](#)]
36. Dai, X.; Zhao, P.X. psRNATarget: A plant small RNA target analysis server. *Nucleic Acids Res.* **2011**, *39*, W155–W159. [[CrossRef](#)]
37. Dai, X.; Zhuang, Z.; Zhao, P.X. psRNATarget: A plant small RNA target analysis server (2017 release). *Nucleic Acids Res.* **2018**, *46*, W49–W54. [[CrossRef](#)]
38. Krzywinski, M.; Schein, J.; Birol, I.; Connors, J.; Gascoyne, R.; Horsman, D.; Jones, S.J.; Marra, M.A. Circos: An information aesthetic for comparative genomics. *Genome Res.* **2009**, *19*, 1639–1645. [[CrossRef](#)]
39. Lorenz, R.; Bernhart, S.; Siederdisen, C.; Tafer, H.; Flamm, C.; Stadler, P.; Hofacker, I. ViennaRNA package 2.0. *Algorithms Mol. Biol.* **2011**, *6*, 26. [[CrossRef](#)]
40. Bernhart, S.H.; Tafer, H.; Mückstein, U.; Flamm, C.; Stadler, P.F.; Hofacker, I.L. Partition function and base pairing probabilities of RNA heterodimers. *Algorithms Mol. Biol.* **2006**, *1*, 3. [[CrossRef](#)] [[PubMed](#)]
41. Gandrud, C. *Reproducible Research with R and RStudio*; Chapman and Hall/CRC: Boca Raton, FL, USA, 2018.
42. German, S.; Candresse, T.; Lanneau, M.; Huet, J.; Pernollet, J.; Dunez, J. Nucleotide sequence and genomic organization of apple chlorotic leaf spot closterovirus. *Virology* **1990**, *179*, 104–112. [[CrossRef](#)] [[PubMed](#)]
43. Sato, K.; Yoshikawa, N.; Takahashi, T. Complete nucleotide sequence of the genome of an apple isolate of apple chlorotic leaf spot virus. *J. Gen. Virol.* **1993**, *74*, 1927–1931. [[CrossRef](#)]
44. Singh, R.M.; Singh, D.; Hallan, V. Movement protein of Apple chlorotic leaf spot virus is genetically unstable and negatively regulated by Ribonuclease E in *E. coli*. *Sci. Rep.* **2017**, *7*, 2133. [[CrossRef](#)] [[PubMed](#)]
45. Satoh, H.; Matsuda, H.; Kawamura, T.; Isogai, M.; Yoshikawa, N.; Takahashi, T. Intracellular distribution, cell-to-cell trafficking and tubule-inducing activity of the 50 kDa movement protein of Apple chlorotic leaf spot virus fused to green fluorescent protein. *J. Gen. Virol.* **2000**, *81*, 2085–2093. [[CrossRef](#)] [[PubMed](#)]
46. Yaegashi, H.; Takahashi, T.; Isogai, M.; Kobori, T.; Ohki, S.; Yoshikawa, N. Apple chlorotic leaf spot virus 50 kDa movement protein acts as a suppressor of systemic silencing without interfering with local silencing in *Nicotiana benthamiana*. *J. Gen. Virol.* **2007**, *88*, 316–324. [[CrossRef](#)] [[PubMed](#)]
47. Isogai, M.; Yoshikawa, N. Mapping the RNA-binding domain on the Apple chlorotic leaf spot virus movement protein. *J. Gen. Virol.* **2005**, *86*, 225–229. [[CrossRef](#)]
48. Yaegashi, H.; Isogai, M.; Tajima, H.; Sano, T.; Yoshikawa, N. Combinations of two amino acids (Ala40 and Phe75 or Ser40 and Tyr75) in the coat protein of apple chlorotic leaf spot virus are crucial for infectivity. *J. Gen. Virol.* **2007**, *88*, 2611–2618. [[CrossRef](#)]
49. Mazeikiene, I.; Siksnianiene, J.B.; Gelvonauskienė, D.; Bendokas, V.; Stanys, V. Prevalence and molecular variability of Apple chlorotic leaf spot virus capsid protein genes in Lithuania. *J. Plant Dis. Prot.* **2018**, *125*, 389–396. [[CrossRef](#)]
50. Zhang, B.; Pan, X.; Cox, S.; Cobb, G.; Anderson, T. Evidence that miRNAs are different from other RNAs. *Cell. Mol. Life Sci. CMLS* **2006**, *63*, 246–254. [[CrossRef](#)]
51. Prabu, G.; Mandal, A.K.A. Computational identification of miRNAs and their target genes from expressed sequence tags of tea (*Camellia sinensis*). *Genom. Proteom. Bioinform.* **2010**, *8*, 113–121. [[CrossRef](#)]
52. Ossowski, S.; Schwab, R.; Weigel, D. Gene silencing in plants using artificial microRNAs and other small RNAs. *Plant J.* **2008**, *53*, 674–690. [[CrossRef](#)]
53. Mathews, D.H.; Sabina, J.; Zuker, M.; Turner, D.H. Expanded sequence dependence of thermodynamic parameters improves prediction of RNA secondary structure. *J. Mol. Biol.* **1999**, *288*, 911–940. [[CrossRef](#)]
54. Niu, Q.-W.; Lin, S.-S.; Reyes, J.L.; Chen, K.-C.; Wu, H.-W.; Yeh, S.-D.; Chua, N.-H. Expression of artificial microRNAs in transgenic *Arabidopsis thaliana* confers virus resistance. *Nat. Biotechnol.* **2006**, *24*, 1420–1428. [[CrossRef](#)] [[PubMed](#)]
55. Ashraf, M.A.; Ali, B.; Brown, J.K.; Shahid, I.; Yu, N. In Silico Identification of Cassava Genome-Encoded MicroRNAs with Predicted Potential for Targeting the ICMV-Kerala Begomoviral Pathogen of Cassava. *Viruses* **2023**, *15*, 486. [[CrossRef](#)] [[PubMed](#)]
56. Mohamed, N.A.; Ngah, N.M.F.N.C.; Abas, A.; Talip, N.; Sarian, M.N.; Hamezah, H.S.; Harun, S.; Bunawan, H. Candidate miRNAs from *Oryza sativa* for Silencing the Rice Tungro Viruses. *Agriculture* **2023**, *13*, 651. [[CrossRef](#)]
57. Ashraf, M.A.; Tariq, H.K.; Hu, X.-W.; Khan, J.; Zou, Z. Computational Biology and Machine Learning Approaches Identify Rubber Tree (*Hevea brasiliensis* Muell. Arg.) Genome Encoded MicroRNAs Targeting Rubber Tree Virus 1. *Appl. Sci.* **2022**, *12*, 12908. [[CrossRef](#)]
58. Ashraf, M.A.; Feng, X.; Hu, X.; Ashraf, F.; Shen, L.; Iqbal, M.S.; Zhang, S. In silico identification of sugarcane (*Saccharum officinarum* L.) genome encoded microRNAs targeting sugarcane bacilliform virus. *PLoS ONE* **2022**, *17*, e0261807. [[CrossRef](#)]
59. Ashraf, M.A.; Ashraf, F.; Feng, X.; Hu, X.; Shen, L.; Khan, J.; Zhang, S. Potential targets for evaluation of sugarcane yellow leaf virus resistance in sugarcane cultivars: In silico sugarcane miRNA and target network prediction. *Biotechnol. Biotechnol. Equip.* **2021**, *35*, 1980–1991. [[CrossRef](#)]
60. Ashraf, F.; Ashraf, M.A.; Hu, X.; Zhang, S. A novel computational approach to the silencing of Sugarcane Bacilliform Guadeloupe A Virus determines potential host-derived MicroRNAs in sugarcane (*Saccharum officinarum* L.). *PeerJ* **2020**, *8*, e8359. [[CrossRef](#)]
61. Gaafar, Y.Z.A.; Ziebell, H. Novel targets for engineering *Physostegia* chlorotic mottle and tomato brown rugose fruit virus-resistant tomatoes: In silico prediction of tomato microRNA targets. *PeerJ* **2020**, *8*, e10096. [[CrossRef](#)]

62. Petchthai, U.; Yee, C.S.L.; Wong, S.-M. Resistance to CymMV and ORSV in artificial microRNA transgenic *Nicotiana benthamiana* plants. *Sci. Rep.* **2018**, *8*, 9958. [[CrossRef](#)]
63. Zhang, D.; Zhang, N.; Shen, W.; Li, J.-F. Engineered artificial microRNA precursors facilitate cloning and gene silencing in arabidopsis and rice. *Int. J. Mol. Sci.* **2019**, *20*, 5620. [[CrossRef](#)]
64. Zhang, N.; Zhang, D.; Chen, S.L.; Gong, B.-Q.; Guo, Y.; Xu, L.; Zhang, X.-N.; Li, J.-F. Engineering artificial microRNAs for multiplex gene silencing and simplified transgenic screen. *Plant Physiol.* **2018**, *178*, 989–1001. [[CrossRef](#)]
65. Yasir, M.; Motawaa, M.; Wang, Q.; Zhang, X.; Khalid, A.; Cai, X.; Li, F. Simple webserver-facilitated method to design and synthesize artificial miRNA gene and its application in engineering viral resistance. *Plants* **2022**, *11*, 2125. [[CrossRef](#)]
66. Ali, I.; Amin, I.; Briddon, R.W.; Mansoor, S. Artificial microRNA-mediated resistance against the monopartite begomovirus Cotton leaf curl Burewala virus. *Virol. J.* **2013**, *10*, 231. [[CrossRef](#)] [[PubMed](#)]
67. Duan, C.-G.; Wang, C.-H.; Fang, R.-X.; Guo, H.-S. Artificial microRNAs highly accessible to targets confer efficient virus resistance in plants. *J. Virol.* **2008**, *82*, 11084–11095. [[CrossRef](#)] [[PubMed](#)]
68. Dweep, H.; Sticht, C.; Gretz, N. In-silico algorithms for the screening of possible microRNA binding sites and their interactions. *Curr. Genom.* **2013**, *14*, 127–136. [[CrossRef](#)] [[PubMed](#)]
69. Thody, J.; Moulton, V.; Mohorianu, I. PAREameters: A tool for computational inference of plant miRNA–mRNA targeting rules using small RNA and degradome sequencing data. *Nucleic Acids Res.* **2020**, *48*, 2258–2270. [[CrossRef](#)]
70. Pinzón, N.; Li, B.; Martinez, L.; Sergeeva, A.; Presumey, J.; Apparailly, F.; Seitz, H. microRNA target prediction programs predict many false positives. *Genome Res.* **2017**, *27*, 234–245. [[CrossRef](#)]
71. Kertesz, M.; Iovino, N.; Unnerstall, U.; Gaul, U.; Segal, E. The role of site accessibility in microRNA target recognition. *Nat. Genet.* **2007**, *39*, 1278–1284. [[CrossRef](#)]
72. Golyshev, V.; Pyshnyi, D.; Lomzov, A. Calculation of Energy for RNA/RNA and DNA/RNA Duplex Formation by Molecular Dynamics Simulation. *Mol. Biol.* **2021**, *55*, 927–940. [[CrossRef](#)]
73. Ghoshal, A.; Shankar, R.; Bagchi, S.; Grama, A.; Chatterji, S. MicroRNA target prediction using thermodynamic and sequence curves. *BMC Genom.* **2015**, *16*, 999. [[CrossRef](#)]
74. Kaja, E.; Szcześniak, M.W.; Jensen, P.J.; Axtell, M.J.; McNellis, T.; Makołowska, I. Identification of apple miRNAs and their potential role in fire blight resistance. *Tree Genet. Genomes* **2015**, *11*, 812. [[CrossRef](#)]
75. Liu, X.-X.; Luo, X.-F.; Luo, K.-X.; Liu, Y.-L.; Pan, T.; Li, Z.-Z.; Duns, G.J.; He, F.-L.; Qin, Z.-D. Small RNA sequencing reveals dynamic microRNA expression of important nutrient metabolism during development of *Camellia oleifera* fruit. *Int. J. Biol. Sci.* **2019**, *15*, 416. [[CrossRef](#)]
76. Witkos, T.M.; Koscińska, E.; Krzyżosiak, W.J. Practical aspects of microRNA target prediction. *Curr. Mol. Med.* **2011**, *11*, 93–109. [[CrossRef](#)]
77. Niu, F.; Pan, S.; Wu, Z.; Jiang, D.; Li, S. Complete nucleotide sequences of the genomes of two isolates of apple chlorotic leaf spot virus from peach (*Prunus persica*) in China. *Arch. Virol.* **2012**, *157*, 783–786. [[CrossRef](#)] [[PubMed](#)]
78. Zhu, H.; Wang, G.; Hu, H.; Tian, R.; Hong, N. The genome sequences of three isolates of Apple chlorotic leaf spot virus from pear (*Pyrus sp.*) in China. *Can. J. Plant Pathol.* **2014**, *36*, 396–402. [[CrossRef](#)]

Disclaimer/Publisher’s Note: The statements, opinions and data contained in all publications are solely those of the individual author(s) and contributor(s) and not of MDPI and/or the editor(s). MDPI and/or the editor(s) disclaim responsibility for any injury to people or property resulting from any ideas, methods, instructions or products referred to in the content.